

# Comparisons of STS-1 Experimental and Predicted Heating Rates

E. Vincent Zoby\*

*NASA Langley Research Center, Hampton, Virginia*

Experimental windward-ray heating rates measured during entry of the first Space Shuttle Orbiter mission are compared with predicted rates based on engineering and detailed equilibrium-air analyses. The experimental heating rates were reduced from temperature-time histories which are available only for the trajectory period from Mach 11 to touchdown. The experimental heating rates are computed for two measured emissivity data sets. The differences in the experimental heating rates based on the two emissivity data sets are sufficiently large that different interpretations of the STS-1 aerothermal environment may be inferred. A boundary-layer transition criterion, momentum thickness Reynolds number divided by local Mach number, is computed from the limited flight data and the results yield a maximum value of 290 compared to a corresponding ground-test value of 225.

## Nomenclature

$L$	= vehicle length
$M_e$	= local Mach number
$\dot{q}_c$	= convective heating rate
$R_\theta$	= momentum thickness Reynolds number based on local conditions
$U_\infty$	= freestream velocity
$X$	= axial measurement of vehicle
$X_{TR}$	= axial transition location
$\alpha$	= angle of attack
$\rho_\infty$	= freestream density

## Introduction

**A**ERODYNAMIC and aerothermodynamic data measured during re-entry of the Space Shuttle Orbiter provide an invaluable free-flight experimental data base for a winged-lifting vehicle at Earth entry conditions. The analyses of these data with the existing ground-test data base and computational techniques are intended to aid in the design of future advanced transportation systems and in improvements to the present shuttle. The data, which are recorded by an onboard instrumentation system or telemetered after blackout to ground-track stations, include over 200 temperature measurements. An inverse one-dimensional transient heat-transfer analysis,<sup>1</sup> which models the heat conduction within the thermal protection system (TPS) and the surface radiation, is used to compute the convective rates. On the first flight of the Space Shuttle, hereafter referred to as STS-1, the flight recorder malfunctioned. Thus, only flight data telemetered after blackout are available. This data period is from a freestream Mach number of approximately 11.0 (altitude = 53 km) to touchdown.

Although the STS-1 heat-transfer data were not obtained for the high-entry velocity time periods, the experimental data still provide the first opportunity to compare results from reliable prediction methods with free-flight heating data obtained on a winged lifting vehicle at hypersonic flow conditions. For the present investigation, the experimental laminar and turbulent rates measured along the windward-symmetry plane of STS-1 are compared with calculated equilibrium-air results. The engineering<sup>2</sup> and detailed<sup>3</sup> calculation methods are restricted to the windward-symmetry

plane of shuttle-like bodies at angles of attack from 25-45 deg. The experimental and predicted heating rates are compared over a freestream Mach number range from approximately 11.0-7.0. In addition, design criteria, which are used for transition to turbulent flow and were determined from ground-test information, are compared to computed values based on experimentally determined free-flight transition locations.

## Analysis

In this section the analyses used in the heat-transfer data reduction procedure and the prediction techniques are discussed briefly. Also, the procedures used to determine the freestream parameters (pressure, temperature, and density) and trajectory (velocity, angles of attack, and sideslip) are outlined.

## Trajectory

The trajectory reconstruction process<sup>4</sup> utilizes the ground-tracking data and onboard measurements of orbiter inertial attitude, linear accelerations, and angular rates to determine the inertial position, velocity, and attitude of the vehicle from near-orbital altitude to landing. Onboard measurements of linear acceleration and angular rates are integrated from 183 km to touchdown to obtain a trajectory that is constrained in a weighted least-squares sense to fit ground base tracking data. Ground base tracking data provide measurements of range, azimuth, elevation, and Doppler range rate relative to the tracking station. The result is a statistically best estimate of the vehicle entry trajectory (position, velocity, and attitude) in an inertial reference space. Consideration of the rotation and oblate shape of the Earth allows the trajectory information to be transformed into an Earth/atmosphere referenced system. The product of the trajectory reconstruction process is then a best estimated trajectory (BET) of orbiter entry.

## Freestream Parameters

Definition of the state of the atmosphere through which the orbiter has flown is accomplished by a process<sup>5</sup> that combines atmospheric modeling with the direct measurement of atmospheric profiles of pressure, temperature, density, and winds. The atmospheric data which result from balloon and sounding rocket launches are measured from the ground to an altitude of approximately 90 km. These soundings, however, are made only at a few locations; the locations may not be along the orbiter entry ground track, and the time of day of the soundings may not correspond with that of orbiter entry.

Presented as Paper 82-0002 at the AIAA 20th Aerospace Sciences Meeting, Orlando, Fla., Jan. 11-14, 1982; submitted May 24, 1982; revision received Oct. 18, 1982. This paper is declared a work of the U.S. Government and therefore is in the public domain.

\*Aero-Space Technologist, Aerothermodynamics Branch, Space Systems Division. Member AIAA.

Atmospheric data above 90 km are estimated using upper atmospheric models.

The measured and estimated data are then used to define the freestream pressure, density, temperature, and winds along the orbiter entry corridor. The BET determined by trajectory reconstruction defines the time of day and corresponding latitude, longitude, and altitude of orbiter entry. Atmospheric modeling defines the time-of-day and latitude variations in atmospheric properties. The atmospheric data are extrapolated to the orbiter entry corridor in a manner that accounts for the time-of-day and latitude differences between the orbiter entry and the atmospheric soundings.

#### Heat-Transfer Data Reduction

The orbiter development flight instrumentation (DFI) includes thermocouples mounted within the TPS, in thermal contact with the surface coating, at over 200 vehicle surface locations. These measurements provide time histories of TPS surface temperature throughout the entry and are the basis for the determination of convective heating rates. The measured temperature-time histories are smoothed and subjected to an interactive review process to assure that the smoothed data provide an accurate representation of the raw temperature data. An inverse, one-dimensional, transient heat-transfer analysis is used to determine the convective heating rate to the TPS surface.

Unfortunately, orbiter surface-temperature data from STS-1 are available only for those portions of the entry during which the orbiter was in communications contact with ground stations. This was the result of failure of the onboard DFI recorder to operate during entry. Good data were obtained, however, after blackout, from approximately Mach 11.0 (altitude=53 km) to touchdown. Since the technique<sup>1</sup> requires a surface temperature history and a known initial temperature distribution through the TPS at each thermocouple location, simulated temperature data based on laminar heating assumptions and constrained to fit the actual STS-1 flight data were used<sup>1</sup> to fill the large data gap. Also, at the time of data acquisition the temperature-time histories indicated that the boundary-layer transition front was located at approximately 50% of the vehicle length. Since the simulated data were based on laminar heating assumptions, a transient heating analysis was not conducted<sup>1</sup> for temperature measurements obtained at locations beyond the 50% station. The impact on the computed experimental heating rates due to uncertainties in parameters such as the thermal properties of the TPS, the surface emittance, temperature measurements, and the thermocouple depth location has been investigated.<sup>6</sup> For the STS-1 conditions, such uncertainties are reported<sup>1</sup> to contribute a  $\pm 10\%$  error in the measured heating rates.

#### Prediction Methods

##### Detailed

The viscous-shock-layer (VSL) analysis of Moss<sup>3</sup> includes a detailed description of the equilibrium chemistry and transport properties. The analysis provides for ablation injection at the surface and the flow may be either laminar or turbulent. The set of VSL equations is obtained from the steady-state Navier-Stokes equations by retaining terms up to second order in the inverse square root of the Reynolds number. The set of governing equations is then solved as a parabolic set of equations using an implicit finite-difference numerical procedure. This analysis<sup>3</sup> was used to provide "benchmark" calculations for the design of the Galileo probe.

##### Approximate

The approximate heating method<sup>7</sup> uses a rapid inviscid flowfield procedure,<sup>8</sup> laminar and turbulent heating equations that can be computed for constant or variable-entropy edge conditions, and equilibrium-air correlations.<sup>9</sup> Variable-entropy edge conditions are computed at any point

along the body by moving out into the inviscid flowfield a distance equal to the boundary-layer thickness which is also computed by correlation techniques. Laminar and turbulent heating calculations based on the approximate method have been demonstrated<sup>7</sup> to be in good agreement (within approximately 15%) with corresponding VSL results<sup>3</sup> at Earth, Venusian, and outer planet entry conditions. The approximate results are shown<sup>7</sup> also to agree well with a range of ground-test heat-transfer data.

#### Shuttle Application

The flow environment along the windward ray of the shuttle is approximated by using the present computational methods with an equivalent axisymmetric body. The equivalent axisymmetric body is used<sup>2</sup> to model the coordinates of the shuttle windward-symmetry plane at angles of attack (AOA) from 25-45 deg. Resulting heating-rate calculations have been validated<sup>2</sup> for both laminar and turbulent flow conditions by comparison with shuttle experimental ground-test heat-transfer data and results of existing predictions<sup>10,11</sup> at shuttle flight design conditions. These comparisons yield discrepancies of approximately 10-15% and validate the concept of using an equivalent axisymmetric body to model the shuttle windward-symmetry plane flowfield.

#### Results and Discussion

In this section the limited experimental heating rates computed<sup>1</sup> from the thermocouple measurements located along the windward-symmetry plane of STS-1 are compared with corresponding results of approximate and detailed prediction methods. Factors that may affect these comparisons are considered. In addition, a transition criterion computed at experimentally determined free-flight transition locations is compared to similar results for ground-test conditions.

#### Heating Rates

Experimental heating-rate distributions reduced<sup>1</sup> from the thermocouple measurements are presented in Figs. 1a-h. These experimental results represent laminar, transitional, and turbulent free-flight heating data over a range of freestream Mach numbers from approximately 11.0-7.0 and of altitudes from 53-44 km. Note that for each freestream condition two values of the experimental heating rates are presented at each body location. The heating rates are based on two sets of measured emissivity data for the TPS. The procedures for measuring these emissivity values as a function of temperature and the resulting values are presented in Ref. 1. One data set is essentially represented by a constant emissivity value of 0.9 while the other data set is very temperature dependent, e.g., at 1110 K an emissivity value of 0.76 is obtained. However, it was not possible in the present time frame to ascertain the validity of either data set. There did not appear to be any obvious deficiencies of technique in either data set to warrant rejection. The experimental heating rates based on the higher values of emissivity are shown as filled symbols in Figs. 1a-h and the rates based on the low emissivity data set are presented as the open symbols. The largest change (approximately 18%) in the two sets of heating-rates data occurs on the shuttle at  $X/L < 0.1$ , where the windward-symmetry plane surface temperatures are greater than 1000 K. The largest discrepancies in the emissivity data sets are noted at these temperature levels. The  $\pm 10\%$  error range is not shown on the experimental data presented herein for clarity of illustrating the current results.

In Figs. 1a-h the results of the approximate code<sup>2</sup> are compared with the experimental laminar data and the "fully" turbulent data in Figs. 1g and 1h. Initially, the discussion is based on the comparison of predicted values and the experimental rates computed with the high emissivity data set. In general, these experimental heating distributions are shown

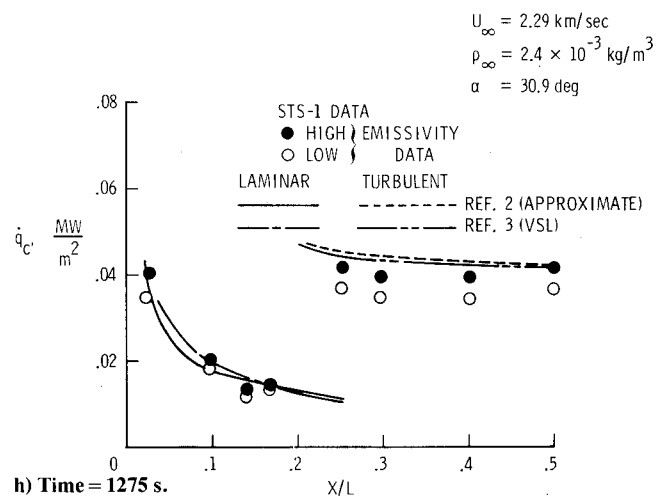
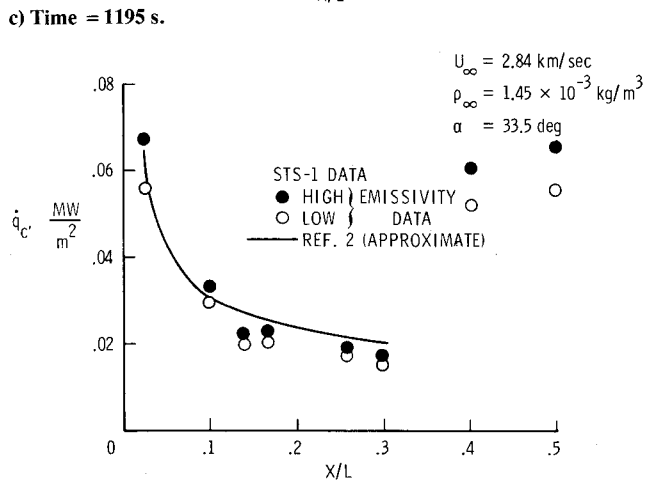
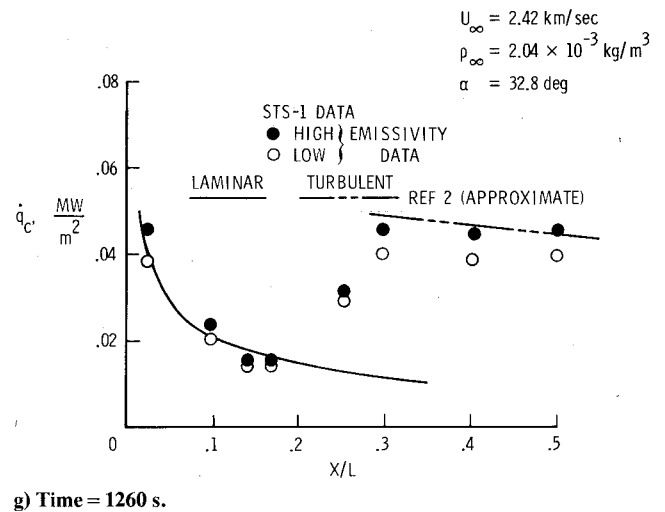
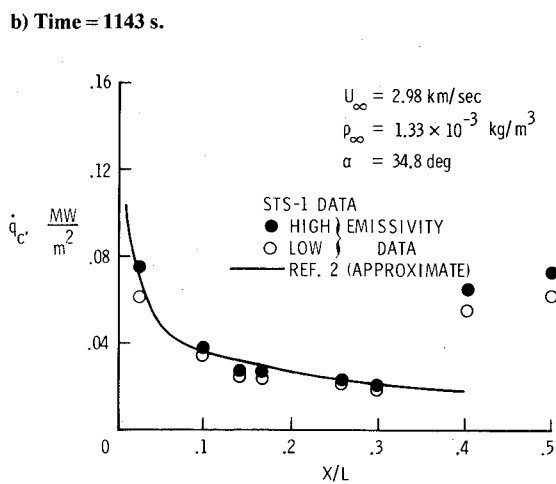
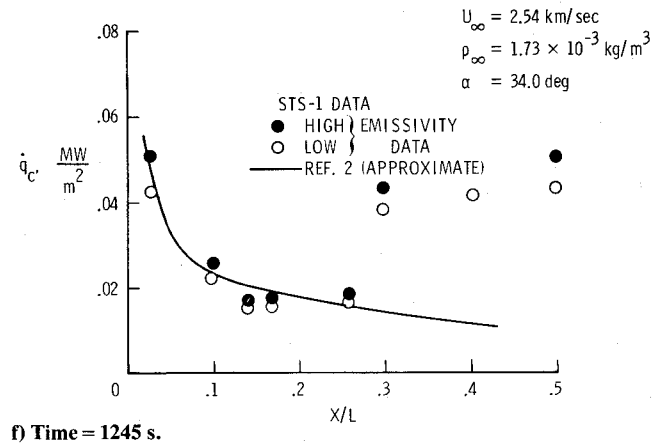
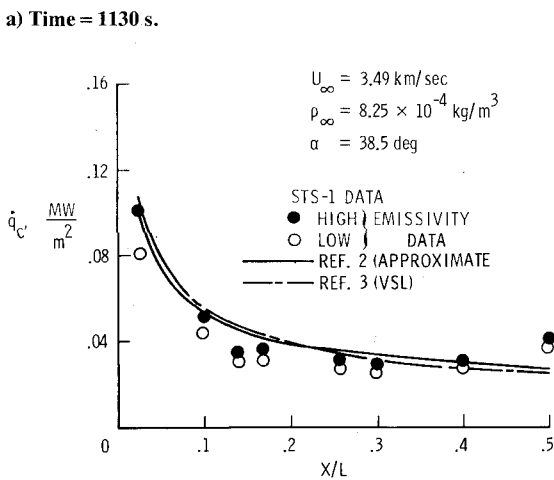
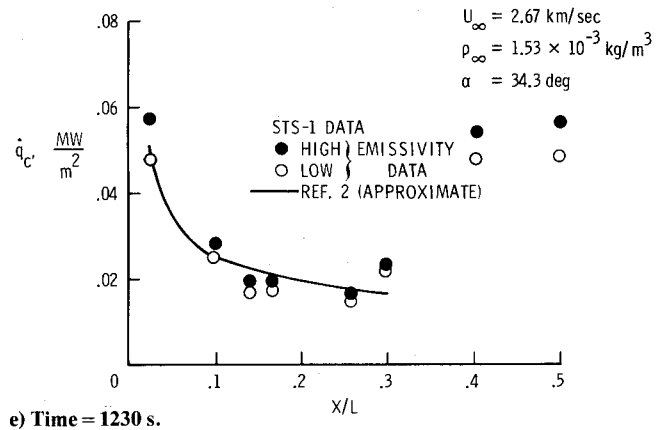
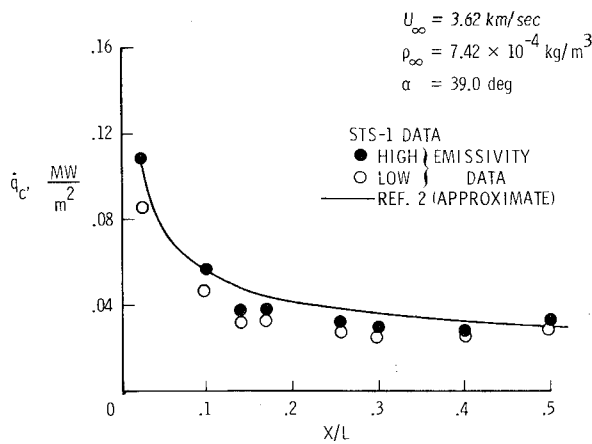


Fig. 1 Comparison of measured and predicted heating rates on STS-1.

to be within 15% of the approximate equilibrium-air predictions. Note that over the region of the shuttle from approximately  $0.15 < X/L < 0.30$ , the laminar experimental data are consistently lower than the corresponding predicted results. Such comparisons of predicted and experimental heating data over this region of the shuttle have been observed in previous investigations<sup>2,12</sup> based on shuttle ground-test data. The computed results of the VSL code<sup>3</sup> are compared in Figs. 1b and 1h and with corresponding turbulent results in Fig. 1h. The VSL results are in good agreement with the approximate results and thus yield similar comparisons with the experimental data. Hence, present approximate and detailed convective heating methods based on equilibrium-air assumptions are in relatively good agreement with the STS-1 experimental heating data reduced with the high emissivity data set. Also, it may be of interest to note that since the STS-1 convective heating is determined primarily from the surface radiation term, the 15% discrepancies in heating-rate comparisons may be discussed as a 4% difference approximately in the computed and measured wall temperatures.

For a comparison of the predicted heating results with the experimental laminar data based on the low emissivity data set (open symbols in Figs. 1a-h) and similar "fully" turbulent data in Figs. 1g and 1h, a different interpretation of the STS-1 aerothermal environment could be inferred. The laminar experimental heating data are shown to be much lower than the predicted results up to an  $X/L$  of 0.3 with discrepancies as large as 25-30%. While such large discrepancies are unsatisfactory, the comparisons do yield an intriguing result. The comparison of the predicted and experimental laminar heating data is observed to improve with decreasing freestream velocity. The stated accuracies in the measured data or the accuracy of the predicted methods would not account for such a trend. A factor that may account for the larger discrepancies as well as for such a trend is the coupling of a finite-reacting flowfield and catalysis of the TPS. Computed heating rates would be lower<sup>13</sup> than corresponding equilibrium values and, at the lower freestream velocities, the gas should be acting as a perfect gas (zero dissociation) so that computed nonequilibrium and equilibrium heating rates approach the same value. The hypothesis for a coupling effect of a nonequilibrium flowfield and surface catalysis at the STS-1 conditions does heighten the interests in the catalytic tile experiment<sup>14</sup> planned for the STS-2 flight. However, for that experiment to be completely beneficial the present uncertainty in the surface emissivity values should be resolved. The comparison of the predicted turbulent results and the experimental data based on the low emissivity data in Figs. 1g and 1h yield differences of 15-20%. These comparisons are at

sufficiently low freestream velocities so that nonequilibrium effects should not be expected. However, a 15-20% difference in comparing predicted and experimental turbulent results is not necessarily unusual.

#### Boundary-Layer Transition

The location of transition to turbulent flow is taken to be the body location where experimental heating rates show a distinct rise from the laminar trend. Local flow properties can be computed at these body locations. A transition criterion ( $R_\theta/M_e$ ), computed at the experimentally determined STS-1 transition locations, is shown as a function of the respective normalized axial transition lengths in Fig. 2. For the STS-1 results, a peak value in  $R_\theta/M_e$  of approximately 290 is computed and the most forward movement of the transition front is located approximately at an  $X/L$  of 0.167.

Ground-test transition results computed in the same parametric form by Goodrich<sup>15</sup> are also represented in Fig. 2. The ground-test data yield a peak value in  $R_\theta/M_e$  of 225. Generally, flight transition Reynolds numbers tend to be greater than ground-test results on similar bodies.<sup>16</sup>

#### Concluding Remarks

Thermocouples are located at over 200 surface locations on the Space Shuttle Orbiter. The temperature-time histories obtained at these measurement stations are available only for the portion of the STS-1 entry when the orbiter was in direct communications with the ground-track stations. This situation resulted from a malfunction in the onboard recorder. The STS-1 data acquisition period begins approximately at a freestream Mach number of 11.0 and an altitude of 53 km. The temperature-time histories have been reduced to heating rates using a transient one-dimensional heat-transfer analysis. An error band of  $\pm 10\%$  has been computed for the STS-1 heating data due to uncertainties in thermal properties as a function of temperature, the temperature measurement, and thermocouple depth location. In addition, the experimental heating rates have been presented based on two sets of measured emissivity data. There is sufficient difference in these measured data at temperatures greater than 1000 K to yield as large as an 18% difference in the experimental heating data at a body location. Also, there does not appear to be justification presently to reject either set of measured emissivity data.

The STS-1 experimental heating rates represent laminar, transition, and turbulent free-flight heating data and are presented over a range of freestream Mach numbers from approximately 11.0-7.0 and of altitudes from 53-44 km. The results of approximate and detailed codes are compared with the experimental laminar and "fully" turbulent data. The predicted results are based on engineering and detailed equilibrium-air analyses. These methods, using an equivalent analytic body, have been demonstrated previously to yield good comparisons (within 10-15%) with ground-test shuttle heat-transfer data and results of existing equilibrium-air prediction techniques at shuttle design trajectory conditions. These comparisons were obtained for both laminar and turbulent flow conditions and at angles of attack from 25-45 deg.

For the experimental heating rates based on the high set of emissivity values, the results of the present laminar and turbulent prediction methods are generally in good agreement (within 15%) with the data. The largest discrepancies occur from  $0.15 < X/L < 0.3$  with the data lower than the predicted results. For the experimental heating rates based on the low set of emissivity values, the comparison of the laminar predicted and experimental results at the higher STS-1 freestream velocity conditions is poor with discrepancies as large as 25-30%. The data are typically lower than the predictions over the first 30% of the vehicle length and the comparisons are shown to improve considerably with

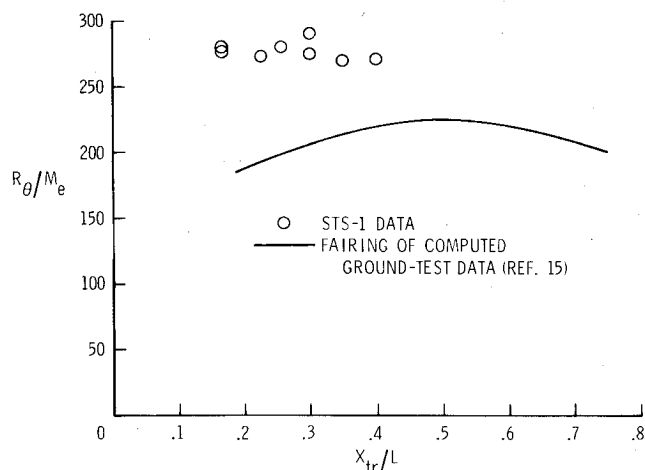


Fig. 2 Comparison of transition criterion at shuttle flight and ground-test conditions.

decreasing freestream velocity. One factor which could account for the larger discrepancies and the trend of the comparisons is the coupling of a finite-reacting flowfield and nonfully catalytic effects of the TPS.

The limited amount of STS-1 boundary-layer-transition data has been compared to a boundary-layer-transition criterion used in shuttle design studies. Local properties are computed at the experimentally determined transition location (experimental rates show distinct rise from the laminar trend) and the parameter, momentum thickness Reynolds number divided by local Mach number, is presented. A peak value of this parameter in the STS-1 results of approximately 290 is compared to a peak value of 225 for ground-test results.

### References

- <sup>1</sup>Throckmorton, D.A., "Benchmark Aeroheating Data from the First Flights of the Space Shuttle Orbiter," AIAA Paper 82-0003, Jan. 1982.
- <sup>2</sup>Zoby, E.V., "Approximate Heating Analysis for the Windward-Symmetry Plane of Shuttle-Like Bodies at Large Angle of Attack," AIAA Paper 81-1042, June 1981; see also, *Thermophysics of Atmospheric Entry*, Progress in Astronautics and Aeronautics, Vol. 82, 1982, pp. 229-247.
- <sup>3</sup>Moss, J.N., "Stagnation and Downstream Viscous Shock Layer Solutions with Radiation and Coupled Ablation Injection," AIAA Paper 74-73, Jan. 1974.
- <sup>4</sup>Compton, H.R., Findlay, J.T., Kelly, G.M., and Heck, M.L., "Shuttle (STS-1) Entry Trajectory Reconstruction," AIAA Paper 81-2459, Nov. 1981.
- <sup>5</sup>Price, J.M. and Blanchard, R.C., "Determination of Atmospheric Properties for STS-1 Aerothermodynamic Investigations," AIAA Paper 81-2430, Nov. 1981.
- <sup>6</sup>Bradley, P.F. and Throckmorton, D.A., "Space Shuttle Orbiter Flight Heating Rate Measurement Sensitivity to Thermal Protection System Uncertainties," NASA TM 83138, June 1981.
- <sup>7</sup>Zoby, E.V., Moss, J.N., and Sutton, K., "Approximate Convective Heating Equations for Hypersonic Flows," AIAA Paper 79-1078, June 1979; see also, *Journal of Spacecraft and Rockets*, Vol. 18, Jan. 1981, pp. 64-70.
- <sup>8</sup>Maslen, S.H., "Inviscid Hypersonic Flow Past Smooth Symmetric Bodies," *AIAA Journal*, Vol. 2, June 1964, pp. 1055-1061.
- <sup>9</sup>Zoby, E.V. and Moss, J.N., "Thermodynamic Equilibrium-Air Correlations for Flowfield Applications," AIAA Paper 81-0280, Jan. 1981; see also, *AIAA Journal*, Vol. 20, June 1982, pp. 849-854.
- <sup>10</sup>Rakich, J.V. and Lanfranco, M.J., "Numerical Computation of Space Shuttle Laminar Heating Surface Streamlines," *Journal of Spacecraft and Rockets*, Vol. 14, May 1977, pp. 565-572.
- <sup>11</sup>Goodrich, W.D., Li, C.P., Houston, C.K., Chiu, P.B., and Olmedo, L., "Numerical Computations of Orbiter Flowfields and Laminar Heating Rates," *Journal of Spacecraft and Rockets*, Vol. 14, May 1977, pp. 257-264.
- <sup>12</sup>Adams, J.C. Jr., Martindale, W.R., and Mayne, A.W. Jr., "Real Gas Scale Effects on Hypersonic Laminar Boundary-Layer Parameters Including Effects of Entropy-Layer Swallowing," AEDC-TR-75-2, Dec. 1975.
- <sup>13</sup>Scott, C.D., "Space Shuttle Laminar Heating With Finite Rate Catalytic Recombination," AIAA Paper 81-1144, June 1981; see also, *Thermophysics of Atmospheric Entry*, Progress in Astronautics and Aeronautics, Vol. 82, 1982, pp. 273-289.
- <sup>14</sup>Stewart, D.A., Rakich, J.V., and Lanfranco, M.J., "Catalytic Surface Effects Experiment on Space Shuttle," AIAA Paper 81-1143, June 1981; see also, *Thermophysics of Atmospheric Entry*, Progress in Astronautics and Aeronautics, Vol. 82, 1982, pp. 248-272.
- <sup>15</sup>Bertin, J.J., Hayden, T.E., and Goodrich, W.D., "Comparison of Correlations of Shuttle Boundary-Layer Transition Due to Distributed Roughness," AIAA Paper 81-8417, Jan. 1981.
- <sup>16</sup>Berkowitz, A.M., Kyriss, C.L., and Martellucci, A., "Boundary Layer Transition Flight Test Observations," AIAA Paper 77-125, Jan. 1977.

## *From the AIAA Progress in Astronautics and Aeronautics Series . . .*

### **REMOTE SENSING OF EARTH FROM SPACE: ROLE OF "SMART SENSORS"—v. 67**

*Edited by Roger A. Breckenridge, NASA Langley Research Center*

The technology of remote sensing of Earth from orbiting spacecraft has advanced rapidly from the time two decades ago when the first Earth satellites returned simple radio transmissions and simple photographic information to Earth receivers. The advance has been largely the result of greatly improved detection sensitivity, signal discrimination, and response time of the sensors, as well as the introduction of new and diverse sensors for different physical and chemical functions. But the systems for such remote sensing have until now remained essentially unaltered: raw signals are radioed to ground receivers where the electrical quantities are recorded, converted, zero-adjusted, computed, and tabulated by specially designed electronic apparatus and large main-frame computers. The recent emergence of efficient detector arrays, microprocessors, integrated electronics, and specialized computer circuitry has sparked a revolution in sensor system technology, the so-called smart sensor. By incorporating many or all of the processing functions within the sensor device itself, a smart sensor can, with greater versatility, extract much more useful information from the received physical signals than a simple sensor, and it can handle a much larger volume of data. Smart sensor systems are expected to find application for remote data collection not only in spacecraft but in terrestrial systems as well, in order to circumvent the cumbersome methods associated with limited on-site sensing.

505 pp., 6×9, illus., \$22.00 Mem., \$42.50 List

TO ORDER WRITE: Publications Dept., AIAA, 1290 Avenue of the Americas, New York, N. Y. 10019